

**Dermal V γ 4⁺ $\gamma\delta$ T cells possess a migratory potency to the draining lymph nodes
and modulate CD8⁺ T cell activity through TNF- α production**

Satoshi Nakamizo¹, Gyohei Egawa¹, Michio Tomura², Shunsuke Sakai³, Soken
Tsuchiya⁴, Akihiko Kitoh¹, Tetsuya Honda^{1,2}, Atsushi Otsuka¹, Saeko Nakajima¹, Teruki
Dainichi¹, Hideaki Tanizaki¹, Masao Mitsuyama³, Yukihiro Sugimoto⁴, Kazuhiro
Kawai⁵, Yasunobu Yoshikai⁶, Yoshiki Miyachi¹, and Kenji Kabashima^{1,7}

¹Department of Dermatology, ²Center for Innovation in Immunoregulative Technology
and Therapeutics, and ³Microbiology, Kyoto University Graduate School of Medicine,
Japan.

⁴Department of Pharmaceutical Biochemistry, Graduate School of Pharmaceutical
Sciences, Kumamoto University, Japan.

⁵Department of Dermatology, Kido Hospital, Niigata, Japan.

⁶Divisions of Host Defense, Medical Institute of Bioregulation, Kyushu University,
Fukuoka, Japan.

⁷PRESTO, Japan Science and Technology Agency, 4-1-8 Honcho, Kawaguchi, Saitama
332-0012, Japan

Correspondence to Kenji Kabashima, MD, PhD, and Gyohei Egawa, MD, PhD

Department of Dermatology, Kyoto University Graduate School of Medicine,
54 Shogoin-Kawahara, Sakyo, Kyoto 606-8507, Japan

Phone: +81-75-751-3310; Fax: +81-75-761-3002

Email address: kaba@kuhp.kyoto-u.ac.jp (K.K.) and gyohei@kuhp.kyoto-u.ac.jp (G.E.)

Short title: Dermal $\gamma\delta$ T cells enhance CD8⁺ T cell response

Abstract

A large number of $\gamma\delta$ T cells are located within epithelial tissues including the skin. In mice, epidermal and dermal $\gamma\delta$ T cells consist of distinct subsets and play specific roles in cutaneous immune responses. A recent study demonstrated that $\gamma\delta$ T cells and cutaneous dendritic cells migrate from the skin to the draining lymph nodes (LNs). However, it remains unclear whether they regulate the antigen-specific immune response within the LNs. Herein, we investigated their properties and role in the LNs using the *Mycobacterium bovis* bacille Calmette-Guérin (BCG) infection model. In vivo cell labeling analysis revealed that the most of migratory subset was dermal $V\gamma 4^+$ cells. This population transmigrated from the skin to the LNs in a Gi-coupled chemokine receptor-independent manner. By depleting $V\gamma 4^+$ cells, the intranodal expansion of $CD8^+$ T cell against BCG was significantly attenuated. In addition, *in vitro* analysis revealed that $V\gamma 4^+$ cells produced TNF- α and enhanced IL-12 production by dendritic cells. Taken together, these findings suggest that dermal $V\gamma 4^+$ cells are a unique subset that possesses a migratory potency to the skin-draining LNs and enhances the dendritic cell function therein.

Introduction

Gamma delta T cells ($\gamma\delta$ T cells) are a minor subset of T cells but are the major T cell population in epithelial tissues, including the skin (Hayday, 2000). In contrast to $\alpha\beta$ T cells, $\gamma\delta$ T cells show less T cell receptor (TCR) diversity and appear to respond to self-molecules that belong to danger signals (Takagaki *et al.*, 1989). Many researchers believe that $\gamma\delta$ T cells function in an innate manner. On activation, $\gamma\delta$ T cells produce a large amount of inflammatory molecules, such as granulocyte-macrophage colony stimulating factor (GM-CSF), interferon (IFN)- γ , and tumor necrosis factor (TNF)- α , and participate in cutaneous immune surveillance (Macleod and Havran, 2011).

In mice, the skin contains at least three subsets of $\gamma\delta$ T cells: epidermal $\gamma\delta$ T cells (also known as dendritic epidermal T cells [DETCs]), dermal $V\gamma 4^+$ cells, and dermal $V\gamma 4^-$ cells (Sumaria *et al.*, 2011). Recent studies emphasize that each subset plays distinct roles in cutaneous immune responses. Strid *et al.* reported that DETCs secrete interleukin (IL)-13 on activation and are involved in the initiation of cutaneous T helper 2 (Th2)-type responses (Strid *et al.*, 2011). DETCs also play an immune-regulatory role in irritant contact dermatitis and allergic contact dermatitis (Girardi *et al.*, 2002). On the other hand, dermal $\gamma\delta$ T cells are known as a main source of IL-17 in mycobacterium infections (Sumaria *et al.*, 2011) and in psoriasiform dermatitis models (Cai *et al.*, 2011; Mabuchi *et al.*, 2011; Yoshiki *et al.*, 2014). These studies suggest that $\gamma\delta$ T cells belong “in between” the innate and adaptive immune systems and can modulate acquired immune responses.

Recently, we demonstrated that some $\alpha\beta$ T cells in the skin and cutaneous dendritic cells (DCs) migrate to the draining lymph nodes (LNs) and modulate immune events therein (Tomura *et al.*, 2010). This observation suggests that the circulation of immune cells between the skin and the draining LNs is a key mechanism for the modulation of cutaneous immunity. As for $\gamma\delta$ T cells, Gray *et al.* reported that $CCR6^+$ $\gamma\delta$ T cells migrated from the skin to the draining LNs in imiquimod-induced skin inflammation (Gray *et al.*, 2013). However, the function of the migratory subset of $\gamma\delta$ T cells remains undetermined.

In the present study, we examined the properties of a migratory subset of $\gamma\delta$ T cells in the *Mycobacterium bovis* bacille Calmette-Guérin (BCG) infection model. Dermal $\gamma\delta$ T

cells are important for host defense against cutaneous BCG infection (Sumaria *et al.*, 2011). We revealed that dermal $V\gamma 4^+$ cells are a unique subset that possesses a migratory potency to the draining LNs and modulate immune responses against BCG infection.

Results

Dermal $\gamma\delta$ T cells migrate from the skin to the draining LNs

We first analyzed the kinetics of cutaneous $\gamma\delta$ T cells that migrated from the skin to the draining LNs. To track cell migration, we used Kaede-transgenic (tg) mice that expressed a photo-convertible Kaede protein throughout the body (Tomura *et al.*, 2010). Before photoconversion, all cutaneous cells in Kaede-tg mice expressed green fluorescence (Kaede-green) (**Fig.1a, left panel**). Upon violet light exposure to the skin, all cutaneous cells immediately turned their fluorescence to red (Kaede-red) (**Fig.1a, right panel**). It should be noted that no detectable skin inflammation was induced by the violet light exposure (Tomura *et al.*, 2010).

Twenty-four hours after the violet light exposure to the footpad, the draining popliteal LNs and non-draining cervical LNs were harvested. In draining LNs, $13.8 \pm 2.1\%$ of $CD11c^+$ DCs and $5.3 \pm 0.4\%$ of $\gamma\delta$ TCR $^+$ cells expressed Kaede-red (**Fig. 1b**), suggesting that these cells migrated from the skin. Almost no Kaede-red $^+$ cells were found in the non-draining LNs ($< 0.1\%$ of $\gamma\delta$ T cells expressed Kaede-red).

We then sought to examine the migratory kinetics of cutaneous $\gamma\delta$ T cells in the inflammatory condition. It is well known that $\gamma\delta$ T cells play an important role in the surveillance of mycobacterial infection (Belmant *et al.*, 1999). We inoculated *Mycobacterium bovis* BCG to the footpad and exposed to the violet light. The numbers of Kaede-red $^+$ $\gamma\delta$ T cells and Kaede-red $^+$ DCs were significantly increased in the draining LNs after BCG infection (**Fig. 1c**). These results suggest that cutaneous $\gamma\delta$ T cells constantly migrate from the skin to the draining LNs and their migration is enhanced upon BCG infection.

To clarify the $\gamma\delta$ T cell migratory ability in other skin inflammation models, we next evaluated the $\gamma\delta$ T cell migration in contact hypersensitivity model with

dinitrofluorobenzene (DNFB) (Honda *et al.*, 2013). The numbers of Kaede-red⁺ $\gamma\delta$ T cells were increased after the challenge of DNFB (**Supplementary Fig.1**). This result suggests that $\gamma\delta$ T cells migration was enhanced not only in the BCG infection but also in other skin inflammation, such as contact hypersensitivity.

Cutaneous $\gamma\delta$ T cell migration to the draining LNs is independent of Gi-coupled chemokine receptors

Next, we investigated the mechanism of the cutaneous $\gamma\delta$ T cell migration to the draining LNs. Previous studies have shown that cutaneous DCs and $\alpha\beta$ T cells migrated to the draining LNs in a CCR7-dependent manner (Bromley *et al.*, 2013; Randolph *et al.*, 2008). To determine the CCR7-dependency of cutaneous $\gamma\delta$ T cell migration, we mated Kaede-tg mice with CCR7-deficient mice. As previously reported (Bromley *et al.*, 2013), Kaede-red⁺ CD11c⁺ DCs were almost absent in the skin-draining LNs of CCR7-deficient mice (**Fig. 2a, b**). In contrast, the percentage of Kaede-red⁺ $\gamma\delta$ T cells in the draining LNs was comparable irrespective of CCR7-deficiency (**Fig. 2a, b**). Consistent with this observation, CCR7 expression was absent in cutaneous $\gamma\delta$ T cells and Kaede-red⁺ skin-derived $\gamma\delta$ T cells (**Fig. 2c**).

We next examined the involvement of the other Gi-coupled chemokine receptors. With subcutaneous injection of pertussis toxin (PTX), a specific Gi inhibitor, Kaede-red⁺ DCs in the draining LNs were significantly decreased, whereas the $\gamma\delta$ T cell migration to the draining LNs was not affected (**Fig. 2d, e**). Taken together, these results suggest that the cutaneous $\gamma\delta$ T cell migration toward the LNs is independent of Gi-coupled chemokine receptors, including CCR7.

The migratory subset is exclusively V γ 4⁺ dermal $\gamma\delta$ T cells

To further characterize the migratory property of cutaneous $\gamma\delta$ T cells, we examined which $\gamma\delta$ T cell subset participates in the migratory population. In the skin, all DETCs in the epidermis are V γ 5⁺, and dermal $\gamma\delta$ T cells consist of V γ 4⁺, V γ 5⁺ and V γ 4⁻V γ 5⁻ subpopulations (Sumaria *et al.*, 2011). Intriguingly, we found that most of Kaede-red⁺ $\gamma\delta$ T cells in the draining LNs expressed V γ 4, but not V γ 5, in the steady state and after the BCG infection (**Fig. 3a**). This result suggests that V γ 4⁺ dermal $\gamma\delta$ T cells, but not

DETCs possess a capacity to migrate to the draining LNs. Thus, we focused on the V γ 4⁺ cells and examined what percentage of V γ 4⁺ cells in the skin-draining LNs were of skin-origin. Twenty-four hours after photoconversion of the footpad, Kaede-red⁺ cells accounted for 14.5 \pm 5.9% among V γ 4⁺ cells in the popliteal LNs (**Fig. 3b**).

We then compared the surface markers of V γ 4⁺ cells in the dermis and in the skin-draining LNs. As previously reported, dermal V γ 4⁺ cells expressed CCR6 and an E-cadherin ligand CD103 (Gray *et al.*, 2011; Sumaria *et al.*, 2011) (**Fig. 3c**). In the skin-draining LNs, one third of V γ 4⁺ cells were CCR6⁺CD103⁺ (**Fig. 3d**) and the majority of Kaede-red⁺ cells (89.6 \pm 3.1 %) belonged to this population (**Fig. 3e, f**). In turn, Kaede-red⁺ cells accounted for 33.6 \pm 12.0 % of CCR6⁺CD103⁺V γ 4⁺ cells in the popliteal LNs 24 h after photoconversion of the footpad (**Supplementary Fig. 2a**). To evaluate the turnover kinetics of V γ 4⁺ cells in the LNs, we photoconverted the inguinal LNs. Twenty-four hours later, Kaede-red⁺ cells accounted for 50.7 \pm 9.1% in CCR6⁺CD103⁺ V γ 4⁺ cells (**Supplementary Fig. 2b**), suggesting that half of this population was retained in the LNs and the other half was replenished in 24 h. Taken together, these results suggest that the majority of CCR6⁺CD103⁺ V γ 4⁺ cells in skin-draining LNs were of skin-origin. In line with this observation, CCR6⁺CD103⁺ V γ 4⁺ cells were a minor population in the spleen (**Fig. 3f**).

Administration of anti-V γ 4 TCR depleting antibody suppressed CD8⁺ T cell response against BCG infection

We next sought to examine the function of V γ 4⁺ cells in the draining LNs. We evaluated IL-17A and TNF- α expression because dermal $\gamma\delta$ T cells produced these inflammatory cytokines upon activation (**Supplementary Fig. 3**)(Conti *et al.*, 2005; Gray *et al.*, 2013). We found that IL-17A and TNF- α were predominantly expressed by intranodal CCR6⁺CD103⁺ V γ 4⁺ cells in the steady state. (**Fig. 4a**) These results suggest that skin-derived V γ 4⁺ cells are an important source of IL-17A and TNF- α in the draining LNs as well as in the skin.

Next, we examined the role of V γ 4⁺ cells in the intranodal proliferation of antigen-specific CD8⁺ T cells, because CD8⁺ T cells play a pivotal role in the protection

against mycobacterium infection (Winau *et al.*, 2006). Neutralizing anti-V γ 4 antibody- or control antibody-treated mice (**Supplementary Fig. 4**) (Hahn *et al.*, 2004) were transferred with OT-I tg CD8⁺ T cells, which specifically recognizes processed peptide of the ovalbumin protein (OVA). These cells were labeled with Cell Trace Violet (CTV) and their proliferation was evaluated via CTV dilution. OVA-expressing BCG (BCG-OVA) was then inoculated. Depletion of V γ 4⁺ cells significantly reduced the proliferation of OT-I tg CD8⁺ T cells in the draining LNs (**Fig. 4b**). These results suggest that V γ 4⁺ cells are important for the intranodal activation and expansion of antigen-specific CD8⁺ T cells.

V γ 4⁺ cells stimulate antigen-specific CD8⁺ T cell differentiation via modulating DC functions

Immunohistochemical analysis of the draining LNs revealed that $\gamma\delta$ T cells, including Kaede-red⁺ $\gamma\delta$ T cells, were distributed in the interfollicular T cell zone (**Fig. 5a and Supplementary Fig. 5a**), wherein DCs interact with naïve T cells. This observation raised the possibility that skin-derived V γ 4⁺ cells influence $\alpha\beta$ T cells activation via modulating DC functions in the LNs. In fact, such an immunomodulation between $\gamma\delta$ T cells and DCs was reported in a human *in vitro* study (Conti *et al.*, 2005). We therefore compared the properties of intranodal DCs in BCG-infected mice with neutralizing anti-V γ 4 antibody- or control antibody-treatment. No significant difference was observed in the number and co-stimulatory molecule expressions, such as CD80 and CD86, on DCs under a deficiency of V γ 4⁺ cells (**Supplementary Fig. 5b, c**), suggesting that V γ 4⁺ cells contribute little, if any, to the migration and activation of skin-derived DCs.

We next compared the T cell stimulatory properties of intranodal DCs. DCs produce IL-12 that drives CD8⁺ T cell IFN- γ production and differentiation during pathogen infection (Wilson *et al.*, 2008). DCs were isolated from the skin-draining LNs of anti-V γ 4- or control antibody-treated mice 3 days after BCG-OVA infection. These cells were co-cultured with CTV-labeled OT-I tg cells. We observed significant attenuation of OT-I tg cell proliferation (**Fig. 5b**) and impaired production of IFN- γ and IL-12p40 (**Fig. 5c, d**) with depletion of V γ 4⁺ cells. These results indicate that V γ 4⁺ $\gamma\delta$ T cells play an

essential role during the antigen-specific CD8⁺ T cell response against BCG infection possibly via modulating DC functions.

V γ 4⁺ cells stimulate bone marrow-derived DCs to produce IL-12

To further characterize the immune modulation between V γ 4⁺ cells and DCs, we isolated CD4⁺ and V γ 4⁺ cells from naïve mice and co-cultured them with bone marrow-derived DCs (BMDCs). In the presence of V γ 4⁺ T cells, BMDCs produced a higher amount of IL-12 p40 than with the same number CD4⁺ cells (**Fig. 6a, b and Supplementary Fig. 6**), suggesting that V γ 4⁺ $\gamma\delta$ T cells have the potential to activate DCs.

As mentioned in Fig. 4a, skin derived CCR6⁺CD103⁺V γ 4⁺ cells produced a substantial amount of IL-17A and TNF- α . IL-17A and TNF- α are important for DC activation (Papadakis and Targan, 2000; Sutton *et al.*, 2009). Thus, we examined whether IL-17A and/or TNF- α from V γ 4⁺ cells activated DCs. We co-cultured BMDCs with V γ 4⁺ cells in the presence or absence of neutralizing antibody against IL-17A or TNF- α . We found that IL-12 p40 production by BMDCs was not attenuated by the blockade of IL-17A, but was significantly inhibited by the neutralization of TNF- α (**Fig. 6c**). Next, we checked the *in vivo* TNF- α production in the skin draining LNs after BCG infection. We also found that the number of V γ 4⁺ cells producing TNF- α was much higher than that of DCs producing TNF- α in the draining LNs upon BCG infection (**Fig. 6d**). These results suggest that V γ 4⁺ cells stimulate intranodal DCs to produce IL-12p40 via producing TNF- α .

Discussion

In this study, we identify a unique function of dermal $\gamma\delta$ T cells that migrate to the draining LNs. V γ 4⁺ dermal $\gamma\delta$ T cells egressed from the skin to the draining LNs in a Gi-coupled receptor independent manner, and produced IL-17A and TNF- α therein. Following BCG infection, V γ 4⁺ $\gamma\delta$ T cells enhanced CD8⁺ T cell activation in the draining LNs. In addition, V γ 4⁺ cells led to a significant up-regulation of IL-12 production by DCs through a TNF- α -dependent mechanism.

Our previous study showed that cutaneous $\alpha\beta$ T cell migration to the LNs was enhanced upon contact hypersensitivity (Tomura *et al.*, 2010). Herein we have demonstrated that V γ 4⁺ dermal $\gamma\delta$ T cell migration to the LNs is enhanced upon BCG infection. Therefore, cutaneous T cells, as well as DCs, have the potential to accumulate in the LNs, particularly after cutaneous inflammations. The skin-derived regulatory T cells represent a stronger immune regulatory potential than LN-resident populations and play an important role in the resolution of cutaneous inflammation (Tomura *et al.*, 2010). Taken together, our findings suggest that skin-derived T cell is highly-activated in nature and the skin might be an important organ as a site for T cells activation.

The distribution of immune cells is directly affected by the signaling from Gi-coupled chemokine receptors. In cutaneous DCs and $\alpha\beta$ T cells, their migration toward the draining LNs is largely dependent on CCR7 (Bromley *et al.*, 2013). Analysis of skin-draining lymph has demonstrated that bovine $\gamma\delta$ T cells migrated from the skin to the draining lymph nodes in a CCR7 independent manner (Vrieling *et al.*, 2012). Consistently, in this report, we demonstrated that murine V γ 4⁺ dermal $\gamma\delta$ T cell migration to the LNs is independent of Gi-coupled receptors.

Chemokine-independent migration was previously reported in plasma cells in lymphoid follicles (Fooksman *et al.*, 2010). Plasma cells undergo a persistent random walk until they find the medullary cords, where plasma cells are retained by local chemokines for their differentiation. Further studies are required to reveal how dermal $\gamma\delta$ T cells egress from the skin.

Another finding in this study is that skin-derived V γ 4⁺ $\gamma\delta$ T cells participate in intranodal TNF- α production and DC activation. Leslie *et al.* demonstrated that human peripheral blood $\gamma\delta$ T cells interact with human monocyte-derived DCs and induce DC maturation *in vitro* (Leslie *et al.*, 2002). In addition, Conti *et al.* showed that peripheral blood $\gamma\delta$ T cells secrete TNF- α and IFN- γ and activate DC functions (Conti *et al.*, 2005). We and others have shown that V γ 4⁺ $\gamma\delta$ T cells produce TNF- α , but not IFN- γ (Narayan *et al.*, 2012), which suggests that both blood $\gamma\delta$ T cells and skin-derived $\gamma\delta$ T cells activate DCs in a TNF- α -dependent manner. TNF- α is a potent proinflammatory and immunomodulatory cytokine implicated in inflammatory conditions. Treatment with neutralizing anti-TNF- α antibody is effective for several

diseases, including psoriasis, Crohn's disease, and rheumatoid arthritis. However, anti-TNF- α therapy, but not anti-IL-17A therapy, has been linked to an increased risk of granulomatous infections such as tuberculosis (Hueber *et al.*, 2010; Keane *et al.*, 2001). Our study, in line with these clinical observations, suggests that TNF- α is essential for the host response against mycobacterium.

In our examination, the anti-V γ 4 mAb treatment suppressed OT-I proliferation modestly, but significantly reduced the production of IL-12 by DCs, which promotes IFN- γ production by T cells (Okamura *et al.*, 1998). These results suggest that V γ 4⁺ cells modulate the cytokine expression by DCs rather than directly regulate CD8⁺ T cell proliferation.

In conclusion, our study has shown that dermal V γ 4⁺ $\gamma\delta$ T cells play an important role in the draining LNs. V γ 4⁺ $\gamma\delta$ T cells distribute in other epithelial tissues, such as the lung and vagina, and produce IL-17 and TNF- α against infections (Okamoto Yoshida *et al.*, 2010; Rakasz *et al.*, 1998). Thus V γ 4⁺ $\gamma\delta$ T cells might have the capacity to migrate to the draining LNs and augment adaptive immunity via enhancing DC functions in the several epithelial tissues. Clarification of these issues might enable the modulation of systemic immune responses through regulating local immunity.

Materials and Methods

Mice

Seven to ten-week-old C57BL/6N and OT-I tg mice were purchased from SLC (Shizuoka, Japan) and Jackson Laboratory (Bar Harbor, ME), respectively. Kaede-tg, CCR7-deficient, and TCR δ -H2B-eGFP mice were described previously (Forster *et al.*, 1999; Prinz *et al.*, 2006; Tomura *et al.*, 2008). All experimental procedures were approved by the Institutional Animal Care and Use Committee of Kyoto University Graduate School of Medicine.

Antibodies and flow cytometry

Antibodies used in this study were described in Supplementary Table. 1. For intracellular staining, cells were stimulated for 3 h with 50 ng/ml PMA (phorbol myristate acetate; Sigma-Aldrich, St Louis, MO) and 1 μ g/ml ionomycin (Wako, Osaka, Japan) in GolgiStop (BD Biosciences, San Diego, CA), then fixed and permeabilized with Cytofix/Cytoperm buffer (BD Biosciences). Flow cytometry was performed using LSRFortessa (BD Biosciences) and analyzed with FlowJo (TreeStar, San Carlos, CA).

Single cell preparation from ear skin

The ear splits were incubated with 0.25% trypsin/EDTA (Life Technologies, Gaithersburg, MD) for 30 min at 37°C. Then, the epidermis and dermis were separated. Dermis was minced and digested with 1000 U/ml collagenase type II (Worthington Biochemical, Lakewood, NJ) containing 0.1% DNase I (Sigma-Aldrich) for 60 min at 37°C. The cell suspensions were filtered with a 40 μ m cell strainer.

***In vivo* V γ 4⁺ T cell depletion**

Hamster anti-V γ 4 antibody UC3 hybridoma was obtained from American Type Culture Collection (Rockville, MD). V γ 4⁺ cell depletion was achieved by intraperitoneal injection of 200 μ g of anti-V γ 4 antibody 3 days before the BCG infection. Depletion was monitored as previously described (Sumaria *et al.*, 2011).

OT-I tg CD8⁺ T cell isolation, labeling, and adoptive transfer

CD8⁺ T cells were isolated from OT-I tg mice by positive selection using auto MACS (Miltenyi Biotec, Bergisch Gladbach, Germany). CD8⁺ T cell purity was routinely >95% as assessed by flow cytometry. For proliferation assays, purified T cells were labeled with CTV (Life Technologies) according to the manufacturer's protocol. Control or anti-V γ 4 antibody-treated mice received 2×10^6 CTV-labeled OT-I tg CD8⁺ T cells intravenously via the tail vein.

BCG generation and infection

BCG-OVA was generated as described previously (Saito *et al.*, 2006). Mice were anesthetized by isoflurane and 10^6 CFU of BCG suspended in 60 μ l phosphate buffered saline was injected into the footpad. Mice that received CTV-labeled OT-I tg CD8⁺ T cells were infected 24 h after the adoptive transfer of cells. Six days after infection, popliteal LNs were harvested and analyzed by flow cytometry.

Photoconversion and PTX treatment

Photoconversion of the skin was performed (Tomura *et al.*, 2008). Briefly, mice were anesthetized and exposed to violet light at 95 mW/cm² with a 436-nm bandpass filter using Spot UV curing equipment (SP500; USHIO, Tokyo, Japan). For photoconversion of inguinal LNs, Kaede tg mice were anesthetized and the abdominal skin was cut at the midline to visualize the inguinal LNs. The surrounding tissue was covered with aluminum foil, and then the LNs was exposed to violet light through a hole in the foil with continuous instillation of warmed phosphate buffered saline at 37°C. Pertussis toxin (PTX) (1 μ g/mouse; Kaketsuken, Kumamoto, Japan), or phosphate buffered saline was subcutaneously injected into the abdominal skin.

Cell proliferation, beads array and ELISA

For antigen specific CD8 T cell proliferation, OT-I tg CD8⁺ T cells were sorted from the spleen and LNs using auto MACS (Miltenyi Biotec) (purity >95% respectively), and labeled with the CTV. CD11c⁺ DCs were sorted from popliteal LNs 3 days after infection with BCG-OVA using auto MACS (purity >95%) and co-cultured with OT-I tg CD8⁺ T cells. A total of 2×10^5 DCs and 2×10^5 T cells per well were incubated in a 96

well plate for 4 days, and the supernatants were collected for ELISA and beads array assays. The amounts of IFN- γ in the culture medium were measured by enzyme-linked immunosorbent assay (ELISA) (BD Biosciences). The amounts of IL-12 p40 were measured using a cytometric beads array system (BD Biosciences). T cell proliferation was measured by flow cytometric analysis of CTV-labeled cells.

In-vitro culture of BMDCs with V γ 4⁺ cells

Mouse BMDCs were generated as previously described (Otsuka *et al.*, 2011). CD4⁺ and V γ 4⁺ T cells were sorted from naïve murine LNs and the spleen using auto MACS (Miltenyi Biotec). BMDCs (2×10^5) were cultured for 24 h with CD4⁺ or V γ 4⁺ T cells (5×10^4 each) in 96-well round-bottom plates in IL-17RFc (2 μ g/ml; R&D Systems), anti-mouse TNF- α (MP6-XT22) (10 μ g/ml; eBioscience), or control Rat IgG (eBRG1) (10 μ g/ml; eBioscience) antibodies. Golgistop was added for the last 4 h of culture (BD Biosciences).

Statistic analysis

All data were statistically analyzed using Student's *t*-test. *P* value of less than 0.05 was considered to be significant. Bar graphs are presented as mean \pm standard deviation (SD).

Immunohistochemical staining, Quantitative polymerase chain reaction analysis and Contact hypersensitivity protocol

These methods were described in the Supplementary Material and Method.

370 **Acknowledgments**

371 We thank Dr. Takaharu Okada for critical reading of our manuscript. This work was
372 supported in part by Grants-in-Aid for Japan Society for the Promotion of Science of
373 Japan and Precursory Research for Embryonic Science and Technology.

374

References

Belmant C, Espinosa E, Poupot R, *et al.* (1999) 3-Formyl-1-butyl pyrophosphate A novel mycobacterial metabolite-activating human gammadelta T cells. *J Biol Chem* 274:32079-84.

Bromley SK, Yan S, Tomura M, *et al.* (2013) Recirculating memory T cells are a unique subset of CD4+ T cells with a distinct phenotype and migratory pattern. *J Immunol* 190:970-6.

Cai Y, Shen X, Ding C, *et al.* (2011) Pivotal role of dermal IL-17-producing gammadelta T cells in skin inflammation. *Immunity* 35:596-610.

Conti L, Casetti R, Cardone M, *et al.* (2005) Reciprocal activating interaction between dendritic cells and pamidronate-stimulated gammadelta T cells: role of CD86 and inflammatory cytokines. *J Immunol* 174:252-60.

Fooksman DR, Schwickert TA, Victora GD, *et al.* (2010) Development and migration of plasma cells in the mouse lymph node. *Immunity* 33:118-27.

Forster R, Schubel A, Breitfeld D, *et al.* (1999) CCR7 coordinates the primary immune response by establishing functional microenvironments in secondary lymphoid organs. *Cell* 99:23-33.

399 Girardi M, Lewis J, Glusac E, *et al.* (2002) Resident skin-specific gammadelta T cells
400 provide local, nonredundant regulation of cutaneous inflammation. *J Exp Med*
401 195:855-67.
402
403 Gray EE, Ramirez-Valle F, Xu Y, *et al.* (2013) Deficiency in IL-17-committed
404 Vgamma4(+) gammadelta T cells in a spontaneous Sox13-mutant CD45.1(+) congenic
405 mouse substrain provides protection from dermatitis. *Nat Immunol* 14:584-92.
406
407 Gray EE, Suzuki K, Cyster JG (2011) Cutting edge: Identification of a motile
408 IL-17-producing gammadelta T cell population in the dermis. *J Immunol* 186:6091-5.
409
410 Hahn YS, Taube C, Jin N, *et al.* (2004) Different potentials of gamma delta T cell
411 subsets in regulating airway responsiveness: V gamma 1+ cells, but not V gamma 4+
412 cells, promote airway hyperreactivity, Th2 cytokines, and airway inflammation. *J*
413 *Immunol* 172:2894-902.
414
415 Hayday AC (2000) [gamma][delta] cells: a right time and a right place for a conserved
416 third way of protection. *Annu Rev Immunol* 18:975-1026.
417
418 Honda T, Egawa G, Grabbe S, *et al.* (2013) Update of immune events in the murine
419 contact hypersensitivity model: toward the understanding of allergic contact dermatitis.
420 *J Invest Dermatol* 133:303-15.
421
422 Hueber W, Patel DD, Dryja T, *et al.* (2010) Effects of AIN457, a fully human antibody

to interleukin-17A, on psoriasis, rheumatoid arthritis, and uveitis. *Sci Transl Med* 2:52ra72.

Keane J, Gershon S, Wise RP, *et al.* (2001) Tuberculosis associated with infliximab, a tumor necrosis factor alpha-neutralizing agent. *N Engl J Med* 345:1098-104.

Leslie DS, Vincent MS, Spada FM, *et al.* (2002) CD1-mediated gamma/delta T cell maturation of dendritic cells. *J Exp Med* 196:1575-84.

Mabuchi T, Takekoshi T, Hwang ST (2011) Epidermal CCR6+ gammadelta T cells are major producers of IL-22 and IL-17 in a murine model of psoriasiform dermatitis. *J Immunol* 187:5026-31.

Macleod AS, Havran WL (2011) Functions of skin-resident gammadelta T cells. *Cell Mol Life Sci* 68:2399-408.

Narayan K, Sylvia KE, Malhotra N, *et al.* (2012) Intrathymic programming of effector fates in three molecularly distinct gammadelta T cell subtypes. *Nat Immunol* 13:511-8.

Okamoto Yoshida Y, Umemura M, Yahagi A, *et al.* (2010) Essential role of IL-17A in the formation of a mycobacterial infection-induced granuloma in the lung. *J Immunol* 184:4414-22.

Okamura H, Kashiwamura S, Tsutsui H, *et al.* (1998) Regulation of interferon-gamma

production by IL-12 and IL-18. *Curr Opin Immunol* 10:259-64.

Otsuka A, Kubo M, Honda T, *et al.* (2011) Requirement of interaction between mast cells and skin dendritic cells to establish contact hypersensitivity. *PLoS One* 6:e25538.

Papadakis KA, Targan SR (2000) Tumor necrosis factor: biology and therapeutic inhibitors. *Gastroenterology* 119:1148-57.

Prinz I, Sansoni A, Kissenpfennig A, *et al.* (2006) Visualization of the earliest steps of gammadelta T cell development in the adult thymus. *Nat Immunol* 7:995-1003.

Rakasz E, Rigby S, de Andres B, *et al.* (1998) Homing of transgenic gammadelta T cells into murine vaginal epithelium. *Int Immunol* 10:1509-17.

Randolph GJ, Ochando J, Partida-Sanchez S (2008) Migration of dendritic cell subsets and their precursors. *Annu Rev Immunol* 26:293-316.

Strid J, Sobolev O, Zafirova B, *et al.* (2011) The intraepithelial T cell response to NKG2D-ligands links lymphoid stress surveillance to atopy. *Science* 334:1293-7.

Sumaria N, Roediger B, Ng LG, *et al.* (2011) Cutaneous immunosurveillance by self-renewing dermal gammadelta T cells. *J Exp Med* 208:505-18.

Sutton CE, Lalor SJ, Sweeney CM, *et al.* (2009) Interleukin-1 and IL-23 induce innate

IL-17 production from gammadelta T cells, amplifying Th17 responses and autoimmunity. *Immunity* 31:331-41.

Takagaki Y, DeCloux A, Bonneville M, *et al.* (1989) Diversity of gamma delta T-cell receptors on murine intestinal intra-epithelial lymphocytes. *Nature* 339:712-4.

Tomura M, Honda T, Tanizaki H, *et al.* (2010) Activated regulatory T cells are the major T cell type emigrating from the skin during a cutaneous immune response in mice. *J Clin Invest* 120:883-93.

Tomura M, Yoshida N, Tanaka J, *et al.* (2008) Monitoring cellular movement in vivo with photoconvertible fluorescence protein "Kaede" transgenic mice. *Proc Natl Acad Sci U S A* 105:10871-6.

Vrieling M, Santema W, Van Rhijn I, *et al.* (2012) gammadelta T cell homing to skin and migration to skin-draining lymph nodes is CCR7 independent. *J Immunol* 188:578-84.

Wilson DC, Matthews S, Yap GS (2008) IL-12 signaling drives CD8+ T cell IFN-gamma production and differentiation of KLRG1+ effector subpopulations during *Toxoplasma gondii* Infection. *J Immunol* 180:5935-45.

Winau F, Weber S, Sad S, *et al.* (2006) Apoptotic vesicles crossprime CD8 T cells and protect against tuberculosis. *Immunity* 24:105-17.

495

496 Yoshiki R, Kabashima K, Honda T, *et al.* (2014) IL-23 from Langerhans cells is
497 required for the development of imiquimod-induced psoriasis-like dermatitis by
498 induction of IL-17A-producing gammadelta T cells. *J Invest Dermatol* 134:1912-21.

499

500

501

Figure legends

Figure 1. Migration of $\gamma\delta$ T cells from the skin to the draining LN.

(a) Flow cytometry of the skin of Kaede-tg mice before (left) and immediately after (right) the violet light exposure. (b) Flow cytometry of Kaede-red⁺ cells in the draining popliteal LNs 24 h after the photoconversion of the footpad. Cells were gated on CD11c⁺ (left) or $\gamma\delta$ TCR⁺ (right) cells. (c) The number of Kaede-red⁺ CD11c⁺ (left) or $\gamma\delta$ TCR⁺ cells (right) in the draining LNs 3 days after the intra-dermal injection of BCG. The cells in the footpad were photoconverted 24 h before the analysis. Data are representative of three experiments (n=3) and are presented as means \pm SD. * P < 0.05.

Figure 2. $\gamma\delta$ T cells migrate from the skin to the draining LNs in a Gi-independent manner.

(a, b) Flow cytometry of CD11c⁺ (left) and $\gamma\delta$ TCR⁺ (right) cells in the skin-draining LNs of WT (upper panel) and CCR7-deficient (lower panel) Kaede-tg mice 24 h after the photoconversion of the skin. The % frequencies of Kaede-red⁺ cells are shown (b). (c) Flow cytometry of CCR7 expression on V γ 4⁺ T cells in the skin (left panel) and in the skin-draining LN 24 hours after the photoconversion (right panel). (d, e) Flow cytometry of CD11c⁺ (left) and $\gamma\delta$ TCR⁺ (right) cells in the draining LNs of Kaede-tg mice 24 hours after the photoconversion of the skin with PTX- or phosphate buffered saline-treatment. The % frequencies of Kaede-red⁺ cells were shown (e). Data are representative of three experiments (n=3) and are presented as means \pm SD. * P < 0.05.

Figure 3. Skin derived $\gamma\delta$ T cells are V γ 4⁺ dermal $\gamma\delta$ T cells.

(a) Flow cytometric analysis of Kaede-red⁺ $\gamma\delta$ T cells in the draining LNs 24 h after the photoconversion of the skin. The % frequencies of V γ 4⁺ cells are shown in the right panel. (b) Flow cytometric analysis of V γ 4⁺ cells in the skin-draining LNs of Kaede-tg mice 24 h after photoconversion of the skin cells. (c) Flow cytometric analysis of Kaede-red⁺ V γ 4⁺ cells in the dermis. (d) Flow cytometric analysis of V γ 4⁺ cells in the skin-draining LNs. (e) Flow cytometric analysis of Kaede-red⁺ V γ 4⁺ cells in the skin-draining LNs 24 hours after the photoconversion of the skin. (f) The % frequency of CCR6⁺CD103⁺ cells among V γ 4⁺ cells in the dermis, LN, and spleen. Data are

representative of three experiments (n=3), and are presented as means \pm SD.

Figure 4. $V\gamma 4^+$ cells enhance the intranodal expansion of $CD8^+$ T cells against BCG

(a) Relative amount of *Il17a* and *Tnfa* mRNA expression in each subset of intranodal $V\gamma 4^+$ cells. For each subset of $V\gamma 4^+$ cells, equal amounts of total RNA were pooled from five mice. ND, not detected. (b) Flow cytometric analysis of CTV-labeled OT-I tg T cells from control (Ctrl)- or neutralizing anti- $V\gamma 4$ antibody- treated mice 6 days after injection of BCG-OVA. Number of CTV^{low} cells is shown in lower panel. Data are representative of three experiments (n=4) and are presented as means \pm SD. * $P < 0.05$.

Figure 5. $V\gamma 4^+$ $\gamma\delta$ T cells stimulate antigen-specific $CD8^+$ T cell differentiation by enhancement of DC functions.

(a) Immunohistochemical staining of the skin-draining LNs 24 h after the photoconversion of the skin. B220⁺ (white) and $\gamma\delta$ TCR⁺ (green) cells are shown. Right panel shows the higher magnification view of the boxed area in the left panel. Red signals represent Kaede-red. T, T cell zone; B, B cell zone. Arrowheads in the right panel indicate Kaede-red⁺ $\gamma\delta$ T cells (right). Scale bars = 100 μ m (left) and 50 μ m (right). (b-c) The number of CTV^{low} (as an indication of cell proliferation) OT-I tg T cells (b) and IFN- γ producing cells (c). CTV-labeled OT-I tg T cells were cocultured with CD11c⁺ DCs from BCG-OVA-sensitized mice treated with control (Ctrl) or neutralizing anti- $V\gamma 4$ antibody. (d) The protein levels of IFN- γ and IL-12p40 in the coculture supernatant. Data are representative of three experiments (n=3~4) and are presented as means \pm SD. * $P < 0.05$.

Figure 6. $V\gamma 4^+$ $\gamma\delta$ T cells stimulate BMDCs to produce IL-12p40.

(a) The % frequency of IL-12p40⁺ BMDCs cultured with or without $CD4^+$ T cells or $V\gamma 4^+$ cells. (b) The mean fluorescence intensity (MFI) of IL-12p40 expression in BMDCs cultured with or without $V\gamma 4^+$ cells. (c) The % frequency of IL-12p40⁺ BMDCs cultured with or without $V\gamma 4^+$ $\gamma\delta$ T cells in the presence of isotype control (Ctrl), IL-17RFc and anti-TNF- α antibodies. (d) The number of TNF- α^+ CD11c⁺ DCs (open column) and TNF- α^+ $V\gamma 4^+$ cells (filled column) in the skin-draining LNs 3 days after

564 treatment without (day0) or with BCG (day3) Data are representative of three
565 experiments (n = 3) and are presented as means \pm SD. **P* <0.05.

566

567

568

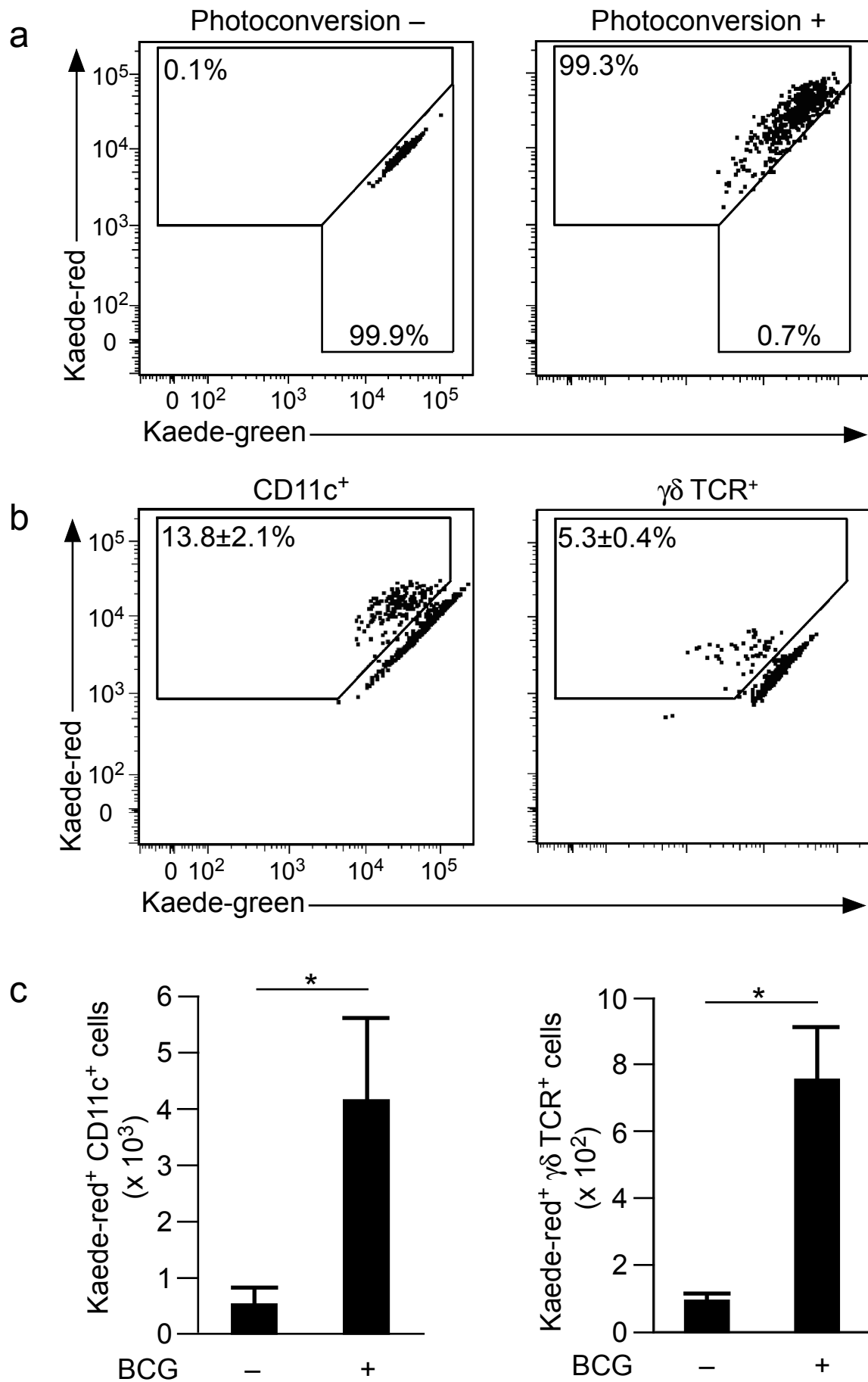


Figure 1

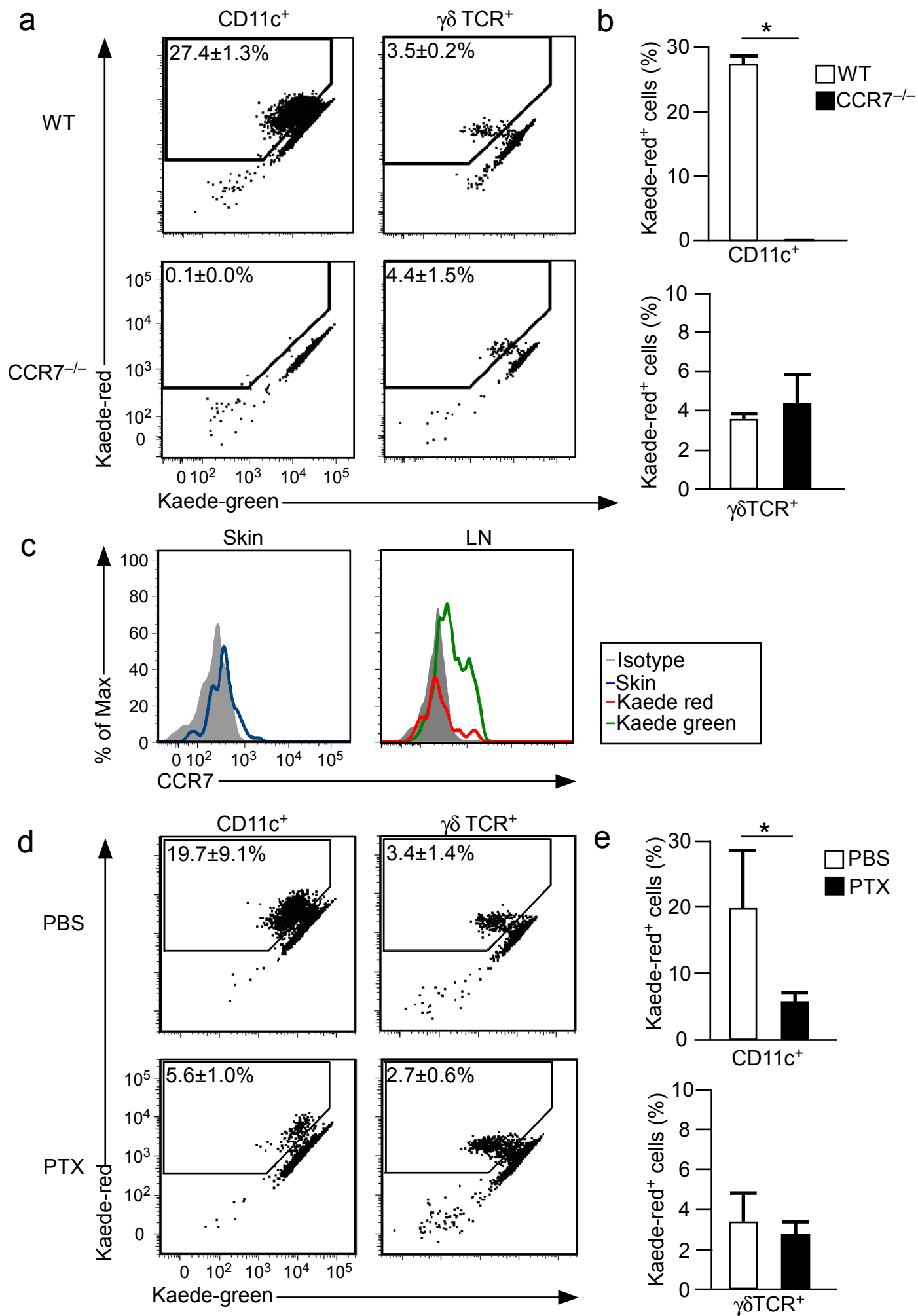


Figure 2

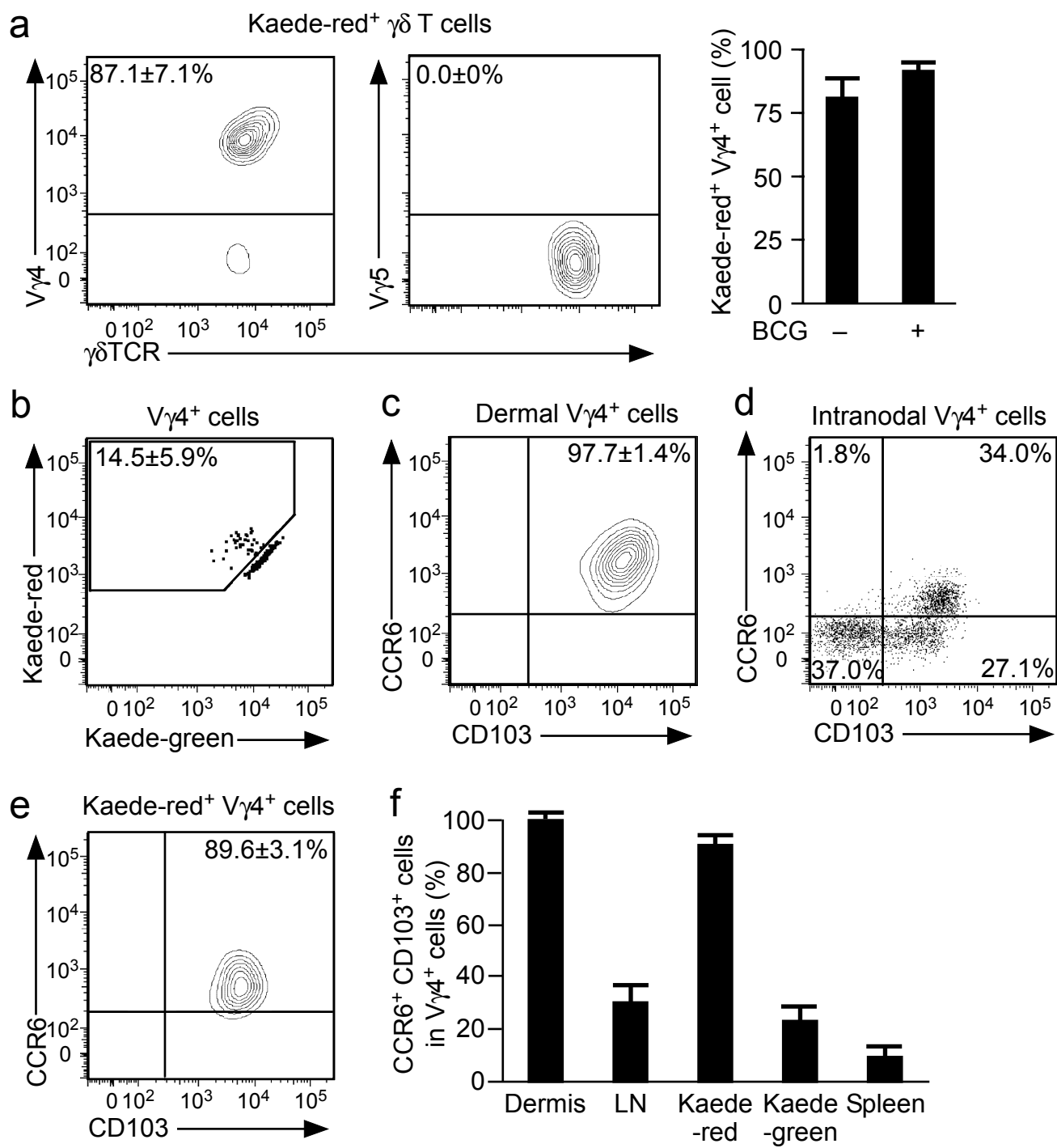


Figure 3

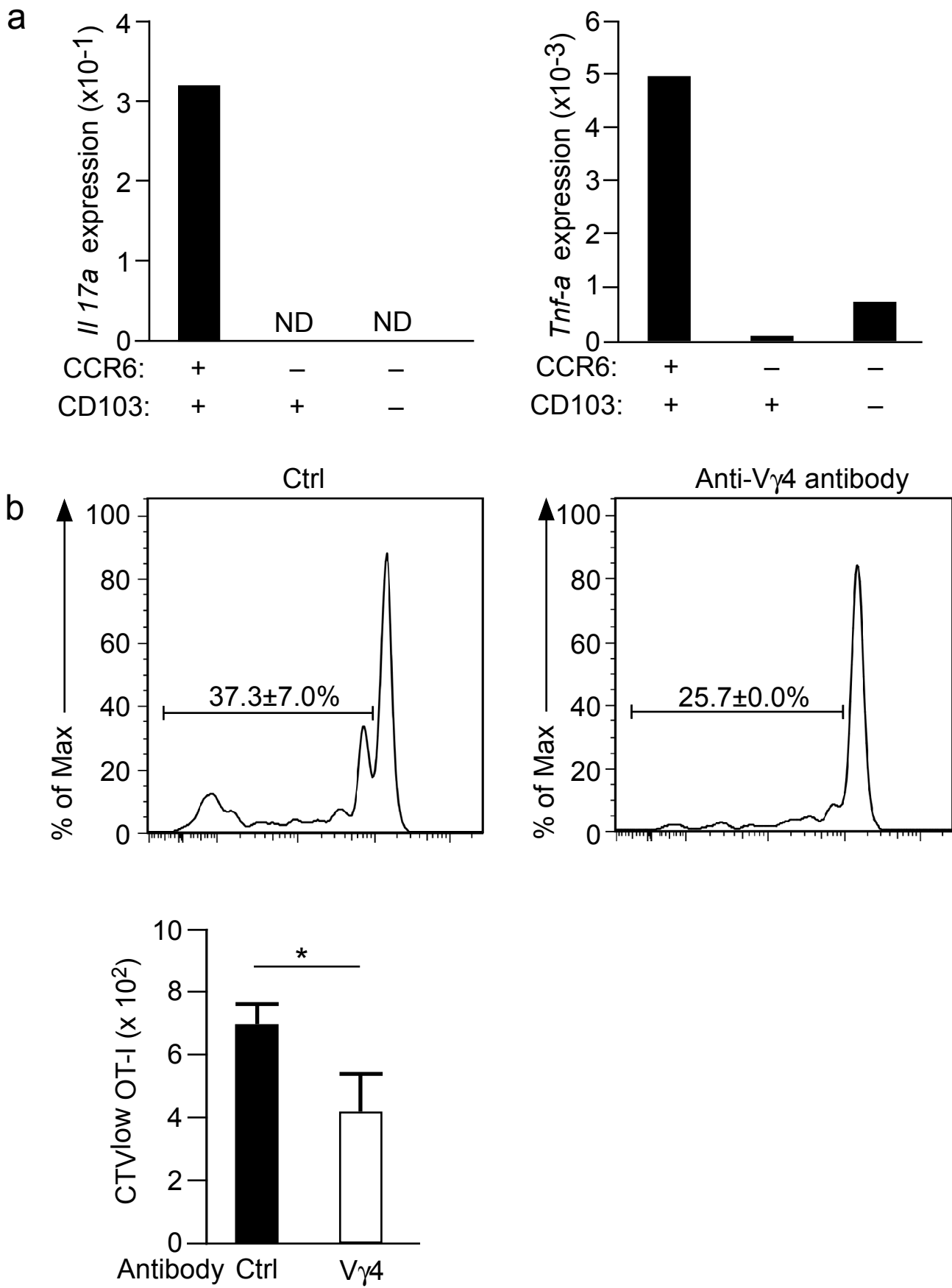


Figure 4

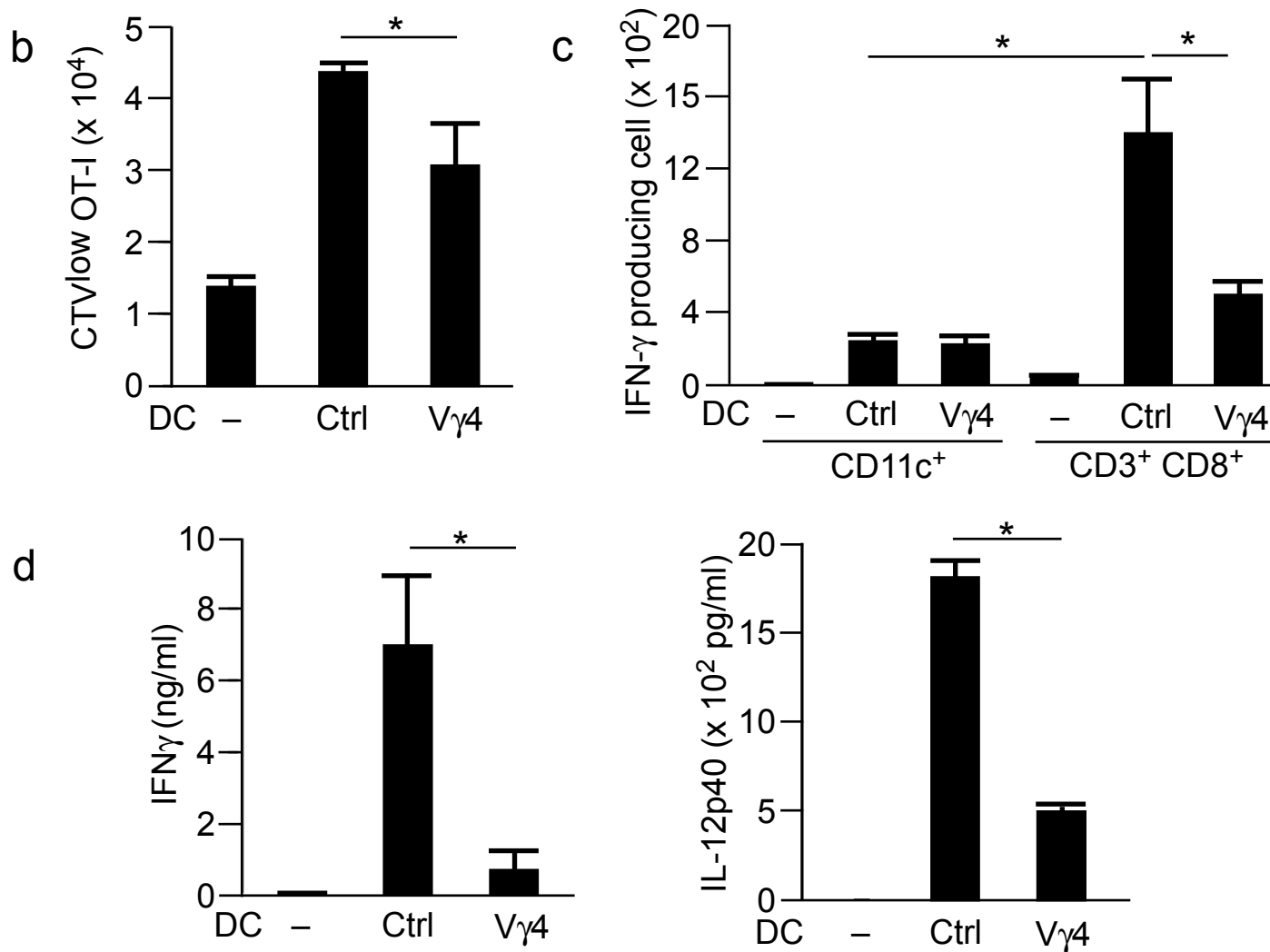
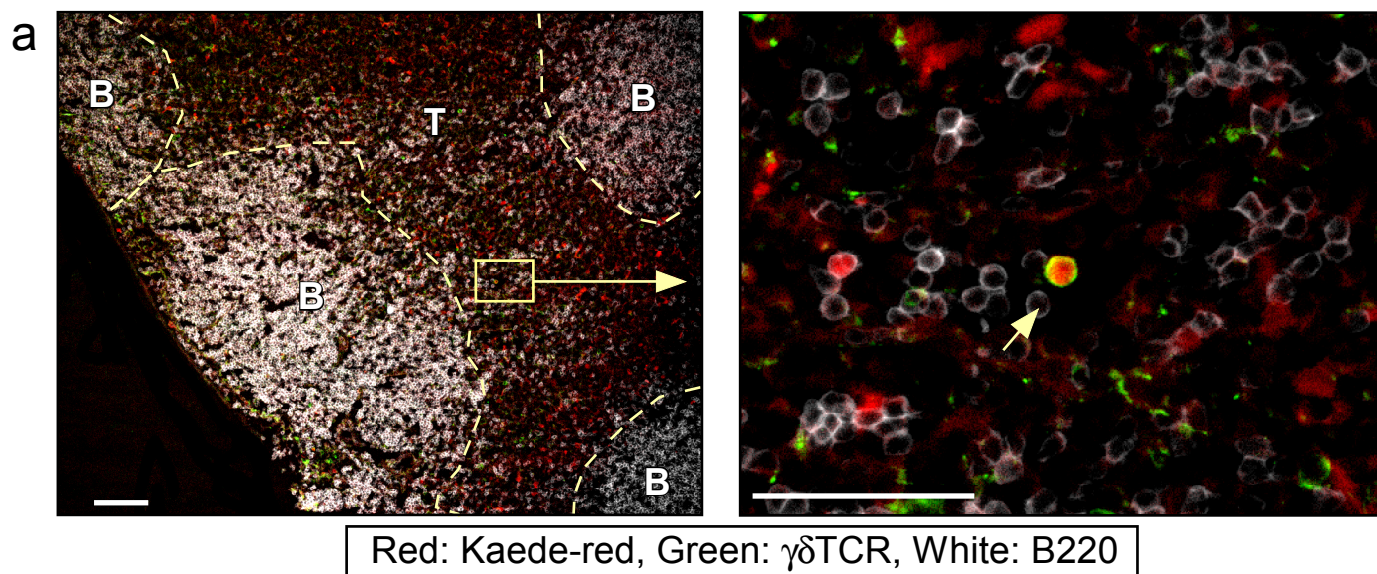


Figure 5

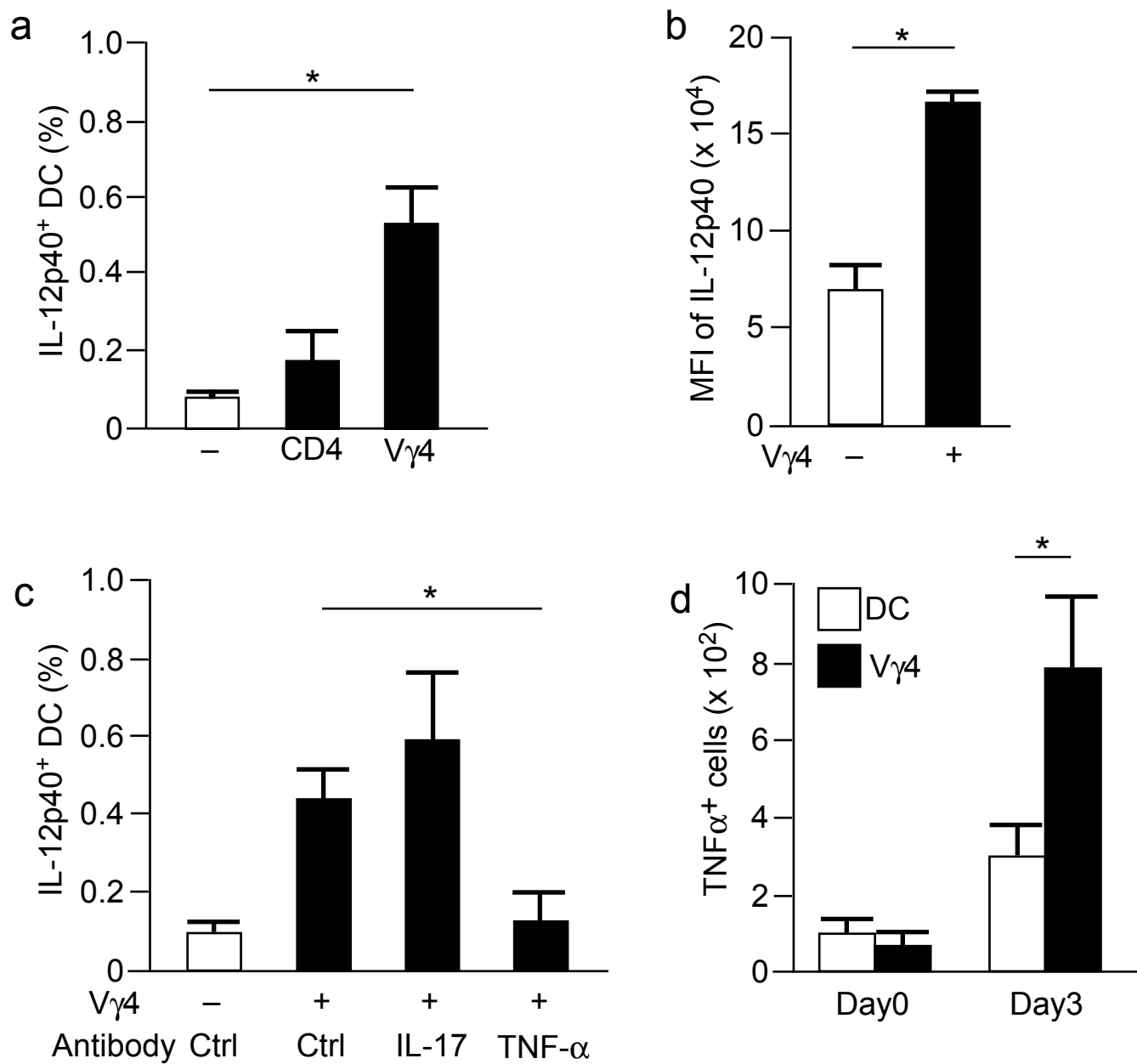


Figure 6

Materials and Methods

Immunohistochemical staining

Immunohistochemical staining of LNs was carried out as described previously (Kabashima *et al.*, 2003). Briefly, LNs samples were immersed in 4% paraformaldehyde (Nacalai Tesque, Kyoto, Japan) for 3 h, embedded in OCT compound (Sakura, Torrance, CA), frozen, and then sectioned. After treatment with Image-iT FX Signal Enhancer (Life Technologies), the sections were incubated with biotin-conjugated anti-mouse $\gamma\delta$ TCR (eBioGL3) (eBioscience), eFluor 450-conjugated anti-mouse B220 (RA3-6B2) (eBioscience), PE-conjugated anti-mouse TCR- β (H57-597) (eBioscience) and APC-conjugated anti-mouse B220 (RA3-6B2) (eBioscience) antibody for 1 h and then with goat anti-rat IgG-Alexa350 and streptavidin -Alexa647 (Life Technologies) for 30 min. The slides were mounted using ProLong Antifade (Life Technologies) and observed under a fluorescent microscope (BZ-900, Keyence, Osaka, Japan).

Quantitative polymerase chain reaction analysis

Cells were sorted with a FACS Aria II cell sorter (BD Biosciences) and total RNA was extracted using a CellAmp Whole Transcriptome Amplification Kit (Takara Bio, Shiga, Japan). Quantitative reverse transcription polymerase chain reaction analysis was performed with SYBR Green I (Roche, Basel, Switzerland) using a Light Cycler 480 (Roche) according to the manufacturer's instructions. The primer sequences used in this study were as follows: Gapdh, 5'- GGCCTCACCCCATTTGATGT -3' (forward) and 5'- CATGTTCCAGTATGACTCCACTC -3' (reverse); IL-17A, 5'- CTCCAGAAGGCCCTCAGACTAC -3' (forward), 5'- GGGTCTTCATTGCGGTGG

-3' (reverse); and TNF- α , 5' - CAGGCGGTGCCTATGTCTC -3' (forward), 5' - CGATCACCCCGAAGTTCAGTAG -3' (reverse). Fold expression was calculated by the $\Delta\Delta C_T$ method and Gapdh was used as a reference gene.

Contact hypersensitivity protocol

The ear of Kaede mice was sensitized with 20 μ l 0.5% (w/v) dinitrofluorobenzene (DNFB; Nacalai Tesque) in acetone/olive oil (4:1) (Nacalai Tesque). Five days after the sensitization, the footpad was challenged with an application of 20 μ l 0.3% DNFB. The number of Kaede-red⁺ $\gamma\delta$ TCR⁺ cells in the draining LNs was measured 3 days after the challenge. The cells in the footpad were photoconverted 24 hours before the analysis.

Supplementary figure legends

Supplementary Figure 1. Skin-derived $\gamma\delta$ T cells into the draining LNs were increased in contact hypersensitivity response.

The number (left) and subset (right) of Kaede-red⁺ $\gamma\delta$ TCR⁺ cells in the draining LNs 3 days after the elicitation. The cells in the footpad were photoconverted 24 h before the analysis. Data are representative of two experiments (n=3) and are presented as means \pm SD.

Supplementary Figure 2. The majority of CCR6⁺ CD103⁺ V γ 4⁺ cells in the LNs are replaced from the skin.

(a) Flow cytometric analysis of CCR6⁺CD103⁺V γ 4⁺ cells in the skin-draining LNs 24 h after the photoconversion of the skin. (b) The % frequency of Kaede-red⁺ V γ 4⁺ cells in the skin-draining LNs of Kaede-tg mice. Data are representative of three experiments (n=3) and are presented as means \pm SD. * $P < 0.05$.

Supplementary Figure 3. V γ 4⁺ $\gamma\delta$ T cells produce IL-17 and TNF- α in the skin

The number of IL-17 (left) and TNF- α (right) producing cells in the skin. Data are representative of three experiments (n=4) and are presented as means \pm SD.

Supplementary Figure 4. Depletion of V γ 4⁺ cells *in vivo*.

FACS plots of skin and LN cells 9 days after anti-V γ 4 or control antibody treatment. The percentages in $\gamma\delta$ TCR⁺ cells were indicated. Data are representative of three experiments (n=4) and are presented as means \pm SD.

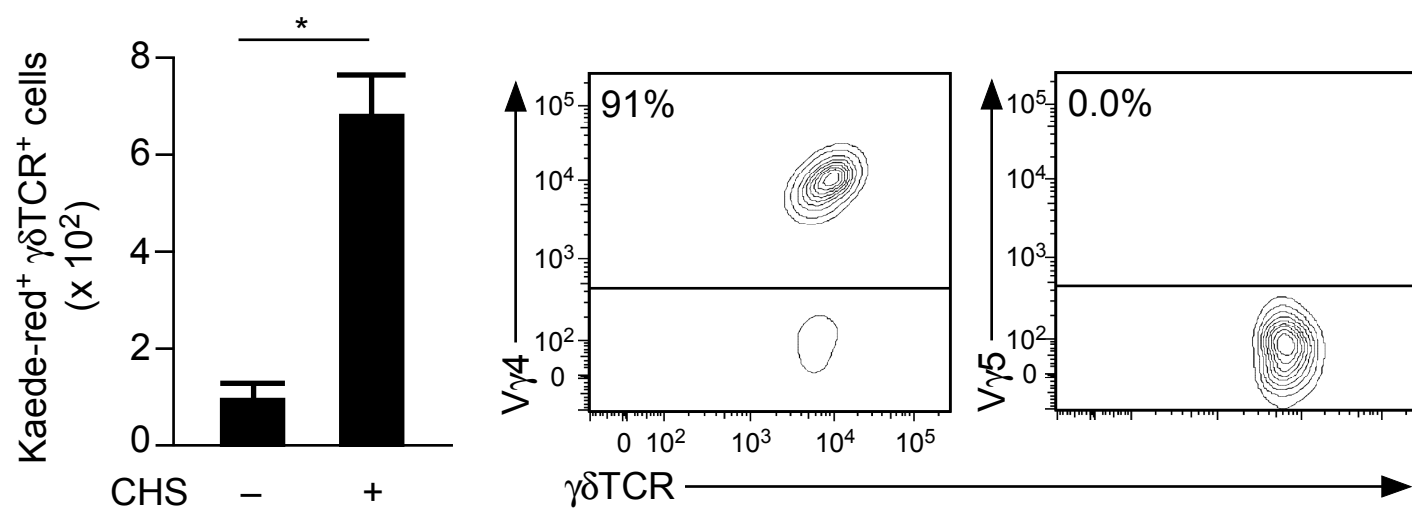
Supplementary Figure 5. $V\gamma 4^+$ cells do not affect migration and activation of DCs.

(a) Immunohistochemical staining of the LNs of TCR δ -H2B-eGFP mice 24 h after the photoconversion of the skin. B220 $^+$ cells (white) and TCR- β^+ cells (red) are shown. Green represents $\gamma\delta$ TCR $^+$ cells. T, T cell zone; B, B cell zone. (b, c) The number (b) and MFI of CD80 and CD86 expression (c) of migratory (MHC II hi CD11c int) and resident (MHC II int CD11c hi) DCs isolated from the draining LNs of control- or anti- $V\gamma 4$ antibody-treated mice 3 days after the inoculation with BCG. Data are representative of three experiments (n=3~4) and are presented as means \pm SD. * P <0.05.

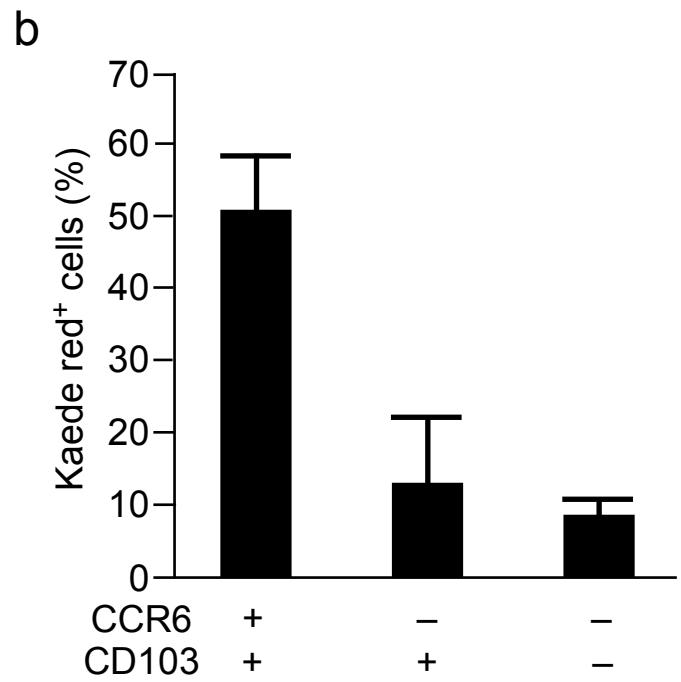
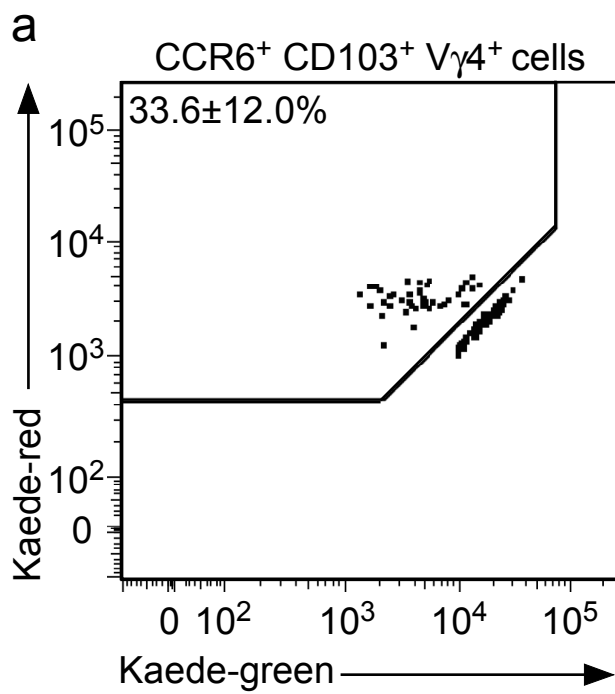
Supplementary Figure 6. $V\gamma 4^+$ $\gamma\delta$ T cells stimulate BMDCs to produce IL-12p40.

FACS plots of IL-12p40 $^+$ BMDCs cultured with or without CD4 $^+$ T cells or $V\gamma 4^+$ cells. Cells were gated on CD11c $^+$ cells. Data are representative of three experiments (n=3).

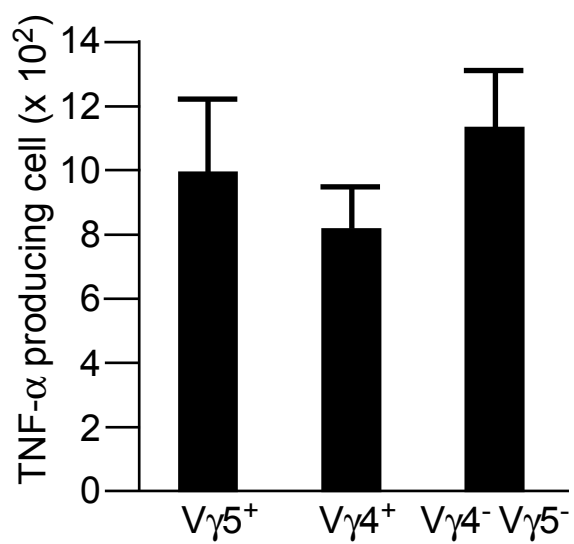
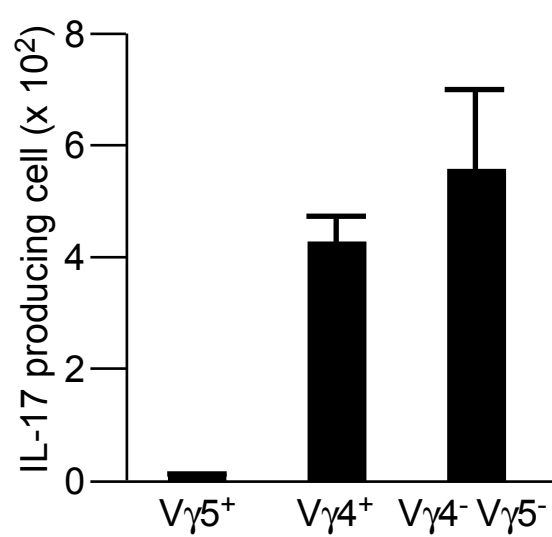
Supplementary Table 1. List of antibodies used in flow cytometry



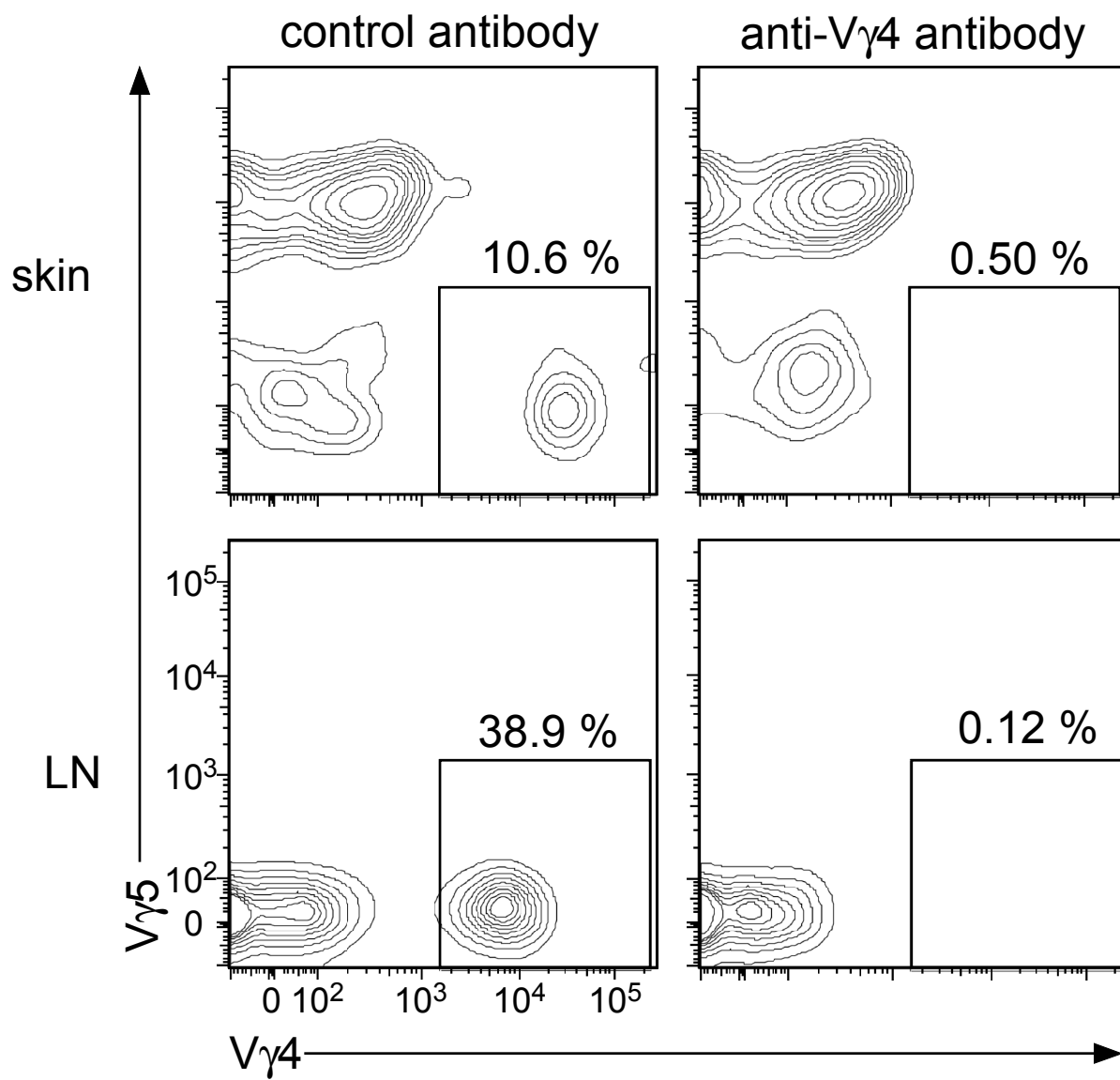
Supplementary Figure 1



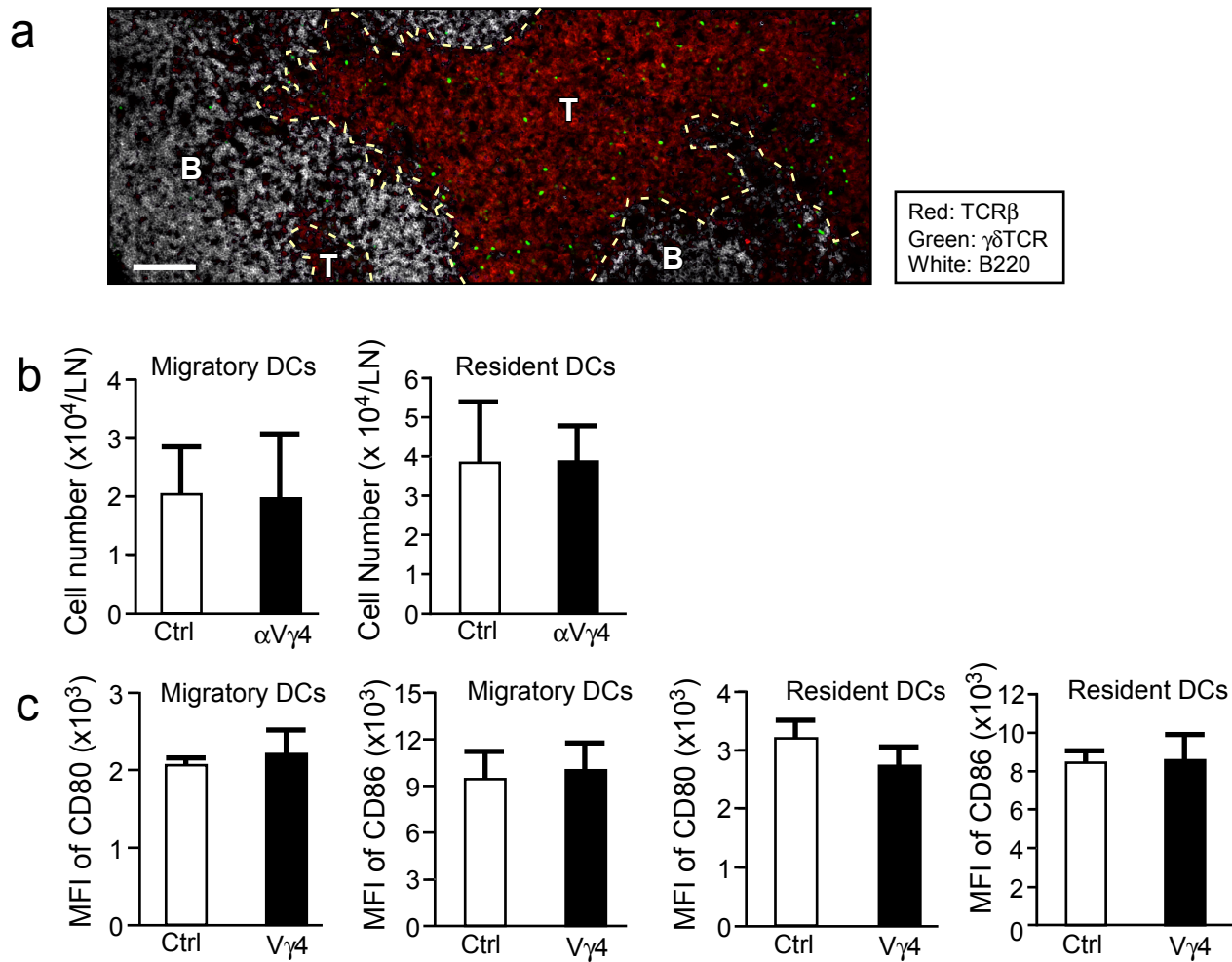
Supplementary Figure 2



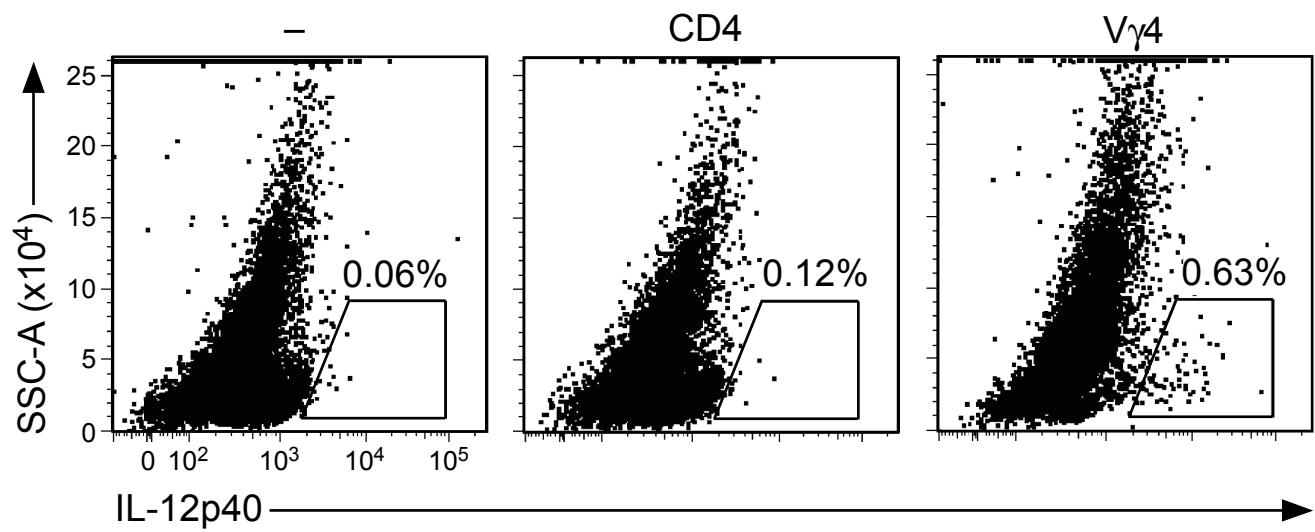
Supplementary Figure 3



Supplementary Figure 4



Supplementary Figure 5



Supplementary Figure 6

List of antibodies used in flow cytometry

Antibodies	Clone	Source
CCR6	29-2L17	BioLegend
CCR7	4B12	eBioscience
CD103	2E7	eBioscience
CD11c	N418	eBioscience
CD3	17A2	BioLegend
CD4	RM4-5	eBioscience
CD45	30-F11	BD Bioscience
CD8a	53.6.7	eBioscience
$\gamma\delta$ TCR	eBioGL3	eBioscience
IFN- γ	XMG1.2	eBioscience
IL-12p40	C17.8	eBioscience
MHC classII	M5/114.15.2	eBioscience
TNF- α	MP6-XT22	eBioscience
V γ 4	UC3-10A6	BioLegend
V γ 5	536	BioLegend

Supplementary Table 1